RESEARCH ARTICLE

Influence of Nano-HA Coated Bone Collagen to Acrylic (Polymethylmethacrylate) Bone Cement on Mechanical Properties and Bioactivity

Tao Li[1], Xisheng Weng[2]*, Yanyan Bian[2], Lei Zhou[2], Fuzhai Cui[3], Zhiye Qiu[3]

1 Department of Orthopedic Surgery, Nanfang Hospital, Southern Medical University, Guangzhou, 510515, PR China, 2 Department of Orthopedic Surgery, Peking Union Medical College Hospital, Peking Union Medical College, Beijing, 100730, PR China, 3 Department of Materials Science and Engineering, Tsinghua University, Beijing, 100087, PR China

* litchn@163.com

Abstract

Objective

This research investigated the mechanical properties and bioactivity of polymethylmethacrylate (PMMA) bone cement after addition of the nano-hydroxyapatite(HA) coated bone collagen (mineralized collagen, MC).

Materials & Methods

The MC in different proportions were added to the PMMA bone cement to detect the compressive strength, compression modulus, coagulation properties and biosafety. The MC-PMMA was embedded into rabbits and co-cultured with MG 63 cells to exam bone tissue compatibility and gene expression of osteogenesis.

Results

15.0%(wt) impregnated MC-PMMA significantly lowered compressive modulus while little affected compressive strength and solidification. MC-PMMA bone cement was biologically safe and indicated excellent bone tissue compatibility. The bone-cement interface crosslinking was significantly higher in MC-PMMA than control after 6 months implantation in the femur of rabbits. The genes of osteogenesis exhibited significantly higher expression level in MC-PMMA.

Conclusions

MC-PMMA presented perfect mechanical properties, good biosafety and excellent biocompatibility with bone tissues, which has profoundly clinical values.

Introduction

Polymethylmethacrylate (PMMA) is an organic polymer material. Because of its good mechanical properties, operating performance and biological inertness[1–4], it is widely used in clinical applications such as vertebroplasty[5], arthroplasty[6, 7] and defect repair[8–10]. After implantation, aseptic loosening and shifting of a prosthesis is an important cause of surgical failure. Aseptic loosening of the prosthesis accounts for 52–55% of revision surgeries[11–13] and occurs most frequently at the cement-bone interface[14].

Several strategies have been employed to improve PMMA-based cement-bone interaction. These strategies have mainly focused on improving the material properties or the biological activity of the bone cement. Studies suggest that a lower elastic modulus can reduce failure rates while reducing stress shielding and graft shear stress[15]. The combined effect can eventually reduce bone tissue absorption, small movement and connective tissue formation at the interface, thereby reducing the risk of aseptic loosening[16–20]. A study by Litsky AS *et al* showed that the aseptic loosening rate significantly decreased after the elastic modulus of a PMMA bone cement was reduced from 2.1GPa to 0.27GPa[16].

Improving the biological activity of bone cement would enhance cement-bone crosslinking, thus reducing the loosening rate[21–24]. In addition, the load transferred at the cement-bone interface is mainly based on direct contact rather than on chemical bond formation. Improving the cement-bone crosslinking increases the contact area of the interface, thus making the load transfer more uniform. *In vivo* experiments by Miller MA *et al.* confirmed these theories. In the experiments, the interface from a retrieved human tibia prosthesis was analyzed; the results indicated that deeper crosslinking could greatly reduce the incidence of loosening[25].

The nano-HA coated bone collagen (mineralized collagen, patent number: ZL01129699.2, MC) is a combination material of recombinant human collagen and nano-hydroxyapatite (HA) that is made *in vitro*[26]. In previous studies, MC showed strong biological and osteogenic activities in bone defect repair[26, 27]. In addition, MC maintained its osteogenic activity after combination with calcium sulfate hemihydrate (CSH)[28–31] or polylactide (PLA)[31–34].

The present research investigates the mechanical properties and bioactivity of PMMA bone cement after the addition of nano-HA-coated bone collagen.

Methods

MC-PMMA bone cement preparation

All samples were prepared in accordance with International Standard (ISO5833[35]). Briefly, MC (Allgens Medical, Beijing) was added to commercial PMMA bone cement (Palacos MV, Heraeus) during the early period of dough phase, and then mixed thoroughly as MC-PMMA group. Commercial bone cement served as control (C-PMMA). After mixing, we set them into stainless steel molds with Φ6×12mm, Φ35×2mm, 5×5×5mm, 5×2×2mm to produce samples with different sizes. All samples were sterilized by 20kGy γ-ray irradiation.

Mechanical properties (compressive strength, compression modulus and solidification)

Five bone cement specimens in each group were tested for compressive strength and compression modulus (Allround, Zwick/Roell, Germany) in accordance to ISO 5833[35].

Dough time and setting time were determined according to ISO 5833[35] and ASTM C191 [36]. We divided the solidification phase into four periods including mixing, waiting, application and setting with commercial PMMA bone cement (Osteopal V and Mendec Spine) as controls.

Biological properties

***In vitro* experiments.** Preparation of material extracts: Samples of 5×5×5mm were submerged into normal saline (NS) and MEM-EBSS cell culture medium (containing 10% horse serum, 1% NEAA, 0.25Mm sodium pyruvate, provided by Cell Resource Center in PUMCH) respectively. After incubation at 37°C for 48h, the samples were adjusted to PH 7.4 and stocked in 4°C.

Cytotoxicity and proliferation test with CCK8 method: In the 96-well culture plates, 100μl MEM-EBSS with $5×10^3$ cells/ml of L929 mouse connective tissue cells (Cell Resource Center in PUMCH) was added except the reference group. 10μl MC-PMMA and C-PMMA extracts were added to experimental group and control group respectively, and 0.1% sterilized phenol was designed as positive control.

The cells were incubated in 37°C, 5% CO_2 and cultured for 1, 3, 5 and 7 days. Then 10μl CcK8 reagent (Dojindo, Japan) was added in each well to measure the absorbance at 450nm (OD_{450}) by the microplate reader (Thermo Multiskan Spectrum, Thermo Scientific, USA) after 2h incubation. The cell relative growth rate (RGR) was calculated by the formula below.

$$RGR = (OD_{test} - OD_R) / (OD_{NC} - OD_R) \times 100\%$$

The cytotoxicity scale (CTS) was evaluated according to ISO 10993 [37].

Hemolysis test: Fresh diluted rabbit blood (8ml fresh rabbit blood and 10ml saline) was used to investigate hemolysis of material extracts. 10mL MC-PMMA and C-PMMA extacts were added to 0.2mL fresh diluted rabbit blood respectively with distilled water as positive control and NS as negative control. After incubated at 37°C for 60min and centrifuged for 5min (2500r/min), the absorbance at 545nm (OD_{545}) for the supernatant was measured to calculate the hemolysis ratio (HR).

$$Hemolysis\,Ratio = (OD_{test} - OD_{NC}) / (OD_{PC} - OD_{NC}) \times 100\%$$

Osteogenesis test: Real-time polymerase chain reaction (RT-PCR) was performed to detect gene expression of osteocalcin (BGLAP), osteonectin (SPARC), collagen -1 (Col1A1) and bone sialoprotein (IBSP). For this experiment, bone cement samples with the size of Φ35×2mm were co-cultured with human osteosarcoma cells (MG 63) in the 6-well plate. After incubation at 37°C, 5% CO_2 for 1, 7 and 14 days, the cells were collected using trypsin EDTA (provided by Cell Resource Center in PUMCH) and washed by PBS buffer.

Then the total RNAs from the collected cells were isolated by Trizol Reagent (Invitrogen Life Technologies, USA). The cDNA from the isolated RNA was reversely transcribed by RevertAid First Strand cDNA Synthesis Kit (Thermo, USA) and subjected to RT-PCR by using FastStart Universal SYBR Green Master (Rox) (Rothe, Switzerland). RT-PCR subjected the samples to the following condition: pre-denaturation 95°C/10 min, run through 40 cycles (denaturation 95°C/15s, annealing and extension 60°C/60s), terminal extension 60°C/5min and then melting analysis from 75°C to 95°C at ramp rate of 1°C /20s. The reference gene was ACTIN. The primers for gene SPARC, IBSP, Col1A1, BGLAP and ACTIN were designed with Primer Premier 5.0 (Canada) and synthesized (Invitrogen Biotechnology Co., LTD).

***In vivo* experiments.** Prior to the experiments, approval was acquired by the Committee on the Use of Live Animals in Teaching and Research of the Peking Union Medical College Hospital. Licence to conduct experiments was issued by Peking University Laboratory Animal Centre. All the animals were operated and sacrificed under general anesthesia with injection of pentobarbital sodium(Sigma, US).

Acute systemic toxicity test (intraperitoneal injection): 30 Kunming mice weighing between 27–32g were divided randomly into two groups. The mice in experimental group and control

group were injected respectively with MC-PMMA extracts and saline at 50ml/kg of body weight by intraperitoneal. Then we observed the general condition of mice (including respiration, body temperature, appetite and movement), weight change and toxic manifestations (such as vomiting, diarrhea, convulsions *et al.*) before administration and 24h, 48h, 72h after administration. The mice were sacrificed in 72 hours by inhaling of excessive carbon dioxide, and their livers and kidneys were further under histological observation. The acute systemic toxicity was evaluated according to ISO 10993[37].

Local reactions and chronic liver and kidney toxicity after implantation: 30 6-week-old SD rats with fasting food and water for 12h before operation were anaesthetized by intraperitoneal injection of 2% pentobarbital sodium at 20mg/kg of body weight. Then a 2cm sagittal incision was made on the scalp from 2cm above the posterior superior iliac spine, the epimysium and muscle fibers were separated along the direction of the gluteus maximus to form a cavity. The $5 \times 2 \times 2$mm MC-PMMA bone cements were implanted in bilateral sizes and the incisions were closed in layers. After 1w, 4w, 7w, 12w and 26w of implantation, the muscle samples were drawn from six rats sacrificed by an intraperitoneal overdose injection of pentobarbital sodium, and under fixation by 4% paraformaldehyde, dehydration, embedment in paraffin, section and HE staining. Then the inflammatory condition and tissue reaction surrounding materials were examined with the light microscope. After 12 weeks of operation, liver and kidney were removed from sacrificed rats and observed in gross and biopsy.

Implantation in rabbit bone tissue: 18 adult New Zealand rabbits weighing 2–3kg were divided randomly into experimental group and control group. After fasting food and water for 12h, the rabbits were anaesthetized by ear vein injection of 3% pentobarbital sodium at 30mg/kg of body weight. Then we fixed the rabbits, cut the hair of the legs, disinfected the skin with chlorhexidine and performed the operation under sterile condition. Then a 2cm sagittal incision was made on the skin of femoral distal end the muscles were separated bluntly to expose medial and lateral femoral condyle. A cylindrical cavity (3mm in diameter and 5mm in depth) was made on the medial femoral condyle by using bone drill and irrigated with saline continuously during the drilling to avoid local high temperature. The rabbits in experimental group were implanted with MC-PMMA bone cements, while those in control group implanted with C-PMMA bone cements. Finally the wounds were sutured with vicryl and conventional feeding was performed after implication.

Micro-CT: The material-embedded rabbit bone tissues were harvested after sacrificed with 100 mg/kg pentobarbital sodium at 4th, 12th and 24th week respectively and imaged with three-dimensional microfocus computed tomography (micro-CT, Siemens Inveon MM Gantry CT, Germany), at a voltage of 60 kV and an electric current of 100μA. The fusion situations between embedded materials and surrounding bone tissues were observed in the images of cross-sectional slices of the samples.

Histological Analysis: 3 New Zealand rabbits from experimental group and control group were sacrificed with 100 mg/kg pentobarbital sodium after 4, 12 and 24 weeks respectively. The material-embedded rabbit bone tissues were harvested, fixed in 4% paraformaldehyde, dehydrated and embedded with resin. A total of 50μm sections were obtained with hard tissue slicer (Leica Cryocut, Germany). And the sections were stained with Van Gieson's staining. The sections were observed under light microscope to assess the bone-cement interface crosslinking situation. The area of bone tissue growing into bone cement was measured by observation of three sections chosen for each sample with Image-Pro Plus 6.0 (Media Cybernetics, USA), then its proportion of the whole bone cement could be calculated. The Affinity Index of bone (AI) [38], which was the proportion of length between bone tissue and bone cement to the total length of the interface, was also measured using Image-Pro Plus 6.0.

Table 1. The compressive strength and compressive modulus of MC-PMMA in different proportions ($\overline{X} \pm$ SD, n = 5).

MC proportion (wt/wt%)	compressive strength(MPa)	compression modulus (GPa)
0	90.53±4.39	1.91±0.08
5.0	90.10±2.90	1.84±0.09
10.0	90.16±2.00	1.52±0.09
15.0	89.30±5.26	1.21±0.12
20.0	88.03±4.74	1.63±0.07

doi:10.1371/journal.pone.0129018.t001

Statistical analysis

Statistical analysis was performed with SPSS17.0. Differences between groups were tested by a one-factor analysis of variance (ANOVA) and differences between two means were examined by t test. P<0.05 was considered statistically significant.

Results

Evaluation of mechanical properties

Compressive strength and compression modulus. The compressive strength and compression modulus of MC-PMMA in different proportions were shown in Table 1. We found that the compressive strength decreased and the compressive modulus declinedwith increasing MC content. 15.0% (wt) impregnated MC-PMMA indicated minimal compressive strength of 89.30 ±5.26MPa and compression modulus of 1.21±0.12GPa, which was higher than the industry standard (no less than 70MPa according to ISO 5833[35] and ASTM F451[39]). 15.0% (wt) impregnated MC-PMMA had the best material properties and was used in the further experiments.

Solidification. The solidification characteristics of MC-PMMA at 23°C were displayed in Fig 1. The mixing period, waiting period, application period and setting period were 1min, 4min, 7min and 12 min respectively with PMMA bone cement (Osteopal V and Mendec Spine) as controls, which suggested that MC-PMMA had no influences on its operation performance.

Evaluation of biosafety

Cytotoxicity and cell proliferation. The growth states in 24h and 5 days after L929 cell subculture were observed. We discovered the cells in all groups except the positive control group were in good condition without cell necrosis debris.

The cell relative growth rate (RGR) with CKK8 method in 1day, 3 days, 5 days and 7 days after L929 cell subculture was calculated. The RGR of MC-PMMA was above 90% in 1st week and with 0–1 cytotoxicity scale, which implied the MC-PMMA had no toxic effect on cells.
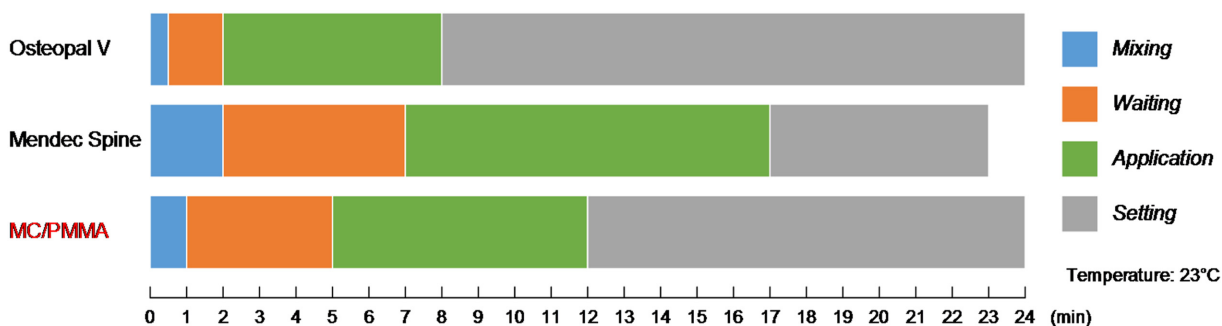

Fig 1. Solidification characteristics of MC-PMMA. Measured at 23°C with PMMA bone cement (Osteopal V, Mendec Sphe) without MC as control.

doi:10.1371/journal.pone.0129018.g001

Blood compatibility test. The 6 tubes in positive control group were red uniformly and no red blood cells were residual in the bottom of the tubes, which illustrated that no hemolysis occurred. All red blood cells in the negative control tubes deposited and the supernatant was clear, which suggested no hemolysis. We observed the similar phenomenon in both MC-PMMA group and C-PMMA group.

The absorbance at 545nm wavelength (OD_{545}) and hemolysis ratio (HR) for different groups were calculated. The HR of MC-PMMA and C-PMMA were 0.26 ± 0.08% and 0.18 ± 0.11% respectively, both of which were less than 5%. Based on the results, it suggested that MC-PMMA and C-PMMA couldn't cause hemolysis.

Short-term acute systemic toxicity. There was no movement decrease, ptosis, difficulty breathing, diarrhea, cyanosis, tremors or any other toxic symptoms happened in the mice before or after intraperitoneal injection of material extracts. The weight change was insignificant ($P > 0.05$). HE staining of liver and kidney at 72h showed normal cell morphology without degeneration or necrosis (S2 Fig).

Local reactions and chronic liver and kidney toxicity after implantation. After implantation for 1, 4, 7, 12 and 26 weeks, the incision healed without infection or abscess. HE staining of the local muscle showed inflammatory cells infiltration at 1 week, and then gradually reduced with fibrous connective tissue formation. A dense fiber wrapped around the material after 12 weeks (S3 Fig). At 12 weeks, HE staining of liver and kidney showed normal cell morphology without degeneration or necrosis (S4 Fig).

Evaluation of bone tissue compatibility. Micro-CT evaluation: Micro-CT evaluation of the samples after implantation for 4, 12 and 24 weeks showed almost no shedding of cement or tiny fracture (Fig 2). The interface was sharp and clear in the C-PMMA group, almost no trabecular ingrowth into the cement. In MC-PMMA group, the surface was similar to that of C-PMMA at 4 weeks, but more and more bone tissue grew into cement from 12 to 24 weeks, forming a better interface interspersed integration.

Histological evaluation: Van Gieson surface staining showed that there was almost no shedding of cement or tiny fracture in any of the sample (Fig 3). There was more bone tissue ingrowth into cement forming a firm anchoring in MC-PMMA and bone insertion depth increased with prolonged implantation.

The bone tissue ingrowth ratios in MC-PMMA group were 7.24±4.46%, 10.95±6.34% and 14.42±9.72% after implantation for 4, 12 and 24 weeks respectively, which were higher than that of C-PMMA group (2.57±1.31%, 2.88±1.20% and 3.14±1.65%, respectively, p<0.05) (Fig 4A). The bone affinity indexes (AI) in MC-PMMA group were 13.10±1.52%, 25.63±1.38% and 34.96±2.33% respectively, significantly higher than the corresponding C-PMMA group (8.94 ±1.47%, 12.21±1.56% and 12.62±1.42%, respectively, p<0.05) (Fig 4B).

Osteogenesis evaluation: The synthesized cDNA from the extracted RNA of the MG63 cells grown in the surface of the samples was used for detecting genes expression. The resulting levels of gene expression were reported as fold change ($2^{-\Delta\Delta Ct}$) in relation to the expression levels recorded from control calibrator group. The result in Fig 5 shows the cellular gene expression of the cells collected from C-PMMA and MC-PMMA samples. After 1 day of incubation, relatively insignificant difference was observed between the two samples across the four primers. The cells from MC-PMMA had depressed expression of BGLAP and higher expressions of SPARC, Col1A1 and IBSP than the cells from C-PMMA after further incubation for 7 and 14 days. Significant differences in the amount of gene expression were observed between C-PMMA and MC-PMMA, especially in the expression of Col1A1 and IBSP after 14 days, wherein MC-PMMA registered a value of (1.03±0.03 and 5.87±0.12 respectively), which was almost double of that of C-PMMA (0.45±0.03 and 2.72±0.90 respectively).
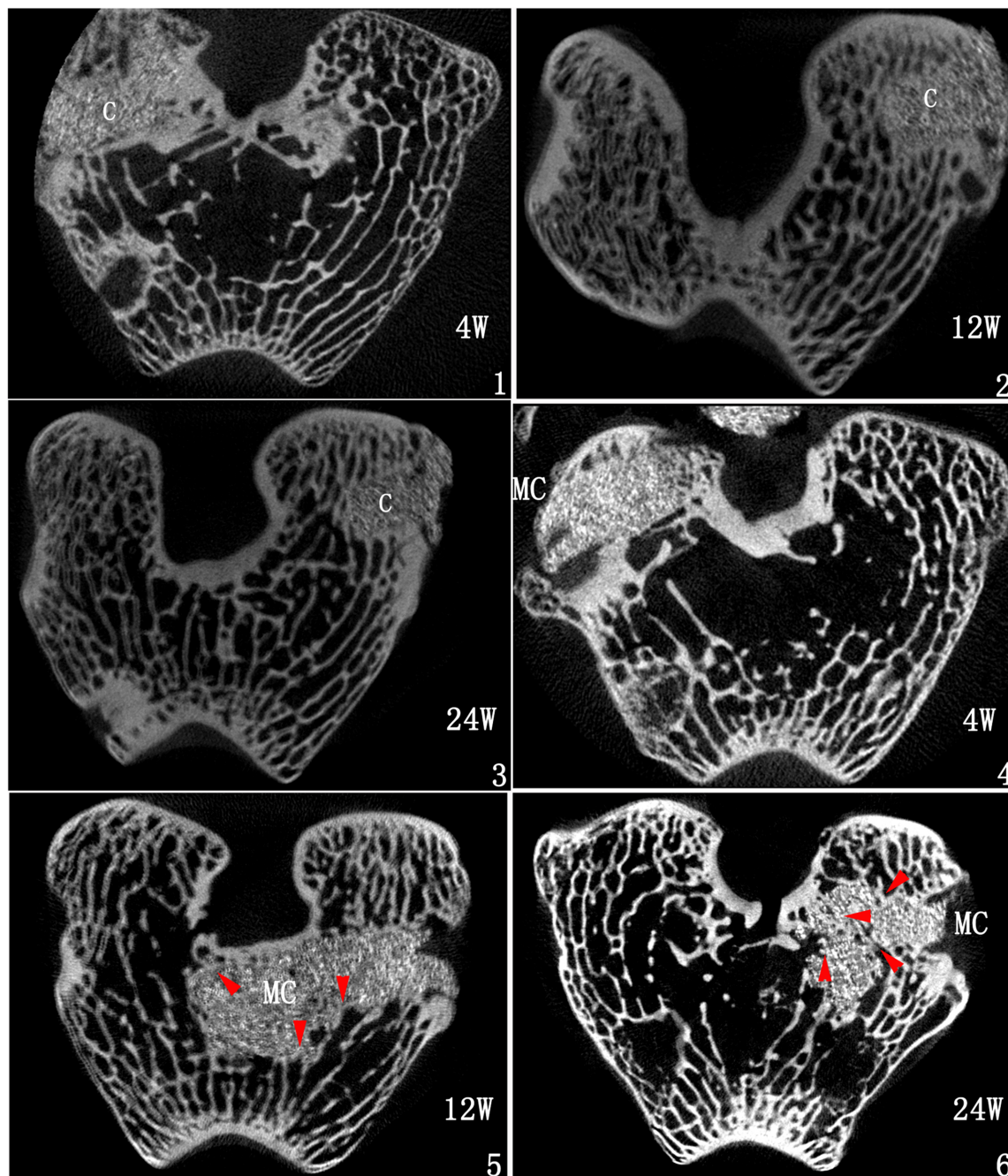
Fig 2. Micro-CT of C-PMMA (1–3) and MC-PMMA (4–6) after implantation for 4 (1,4), 12 (2, 5) and 24 weeks (3, 6). Red arrow indicates the insertion site of trabecular; C, C-PMMA; MC, MC-PMMA.

Discussion

Mechanical properties

Compressive strength, elastic modulus and performance are the most important properties of bone cement. PMMA has outstanding advantages with respect to its compressive strength and operating performance; however, it has the disadvantage of a high elastic modulus, which
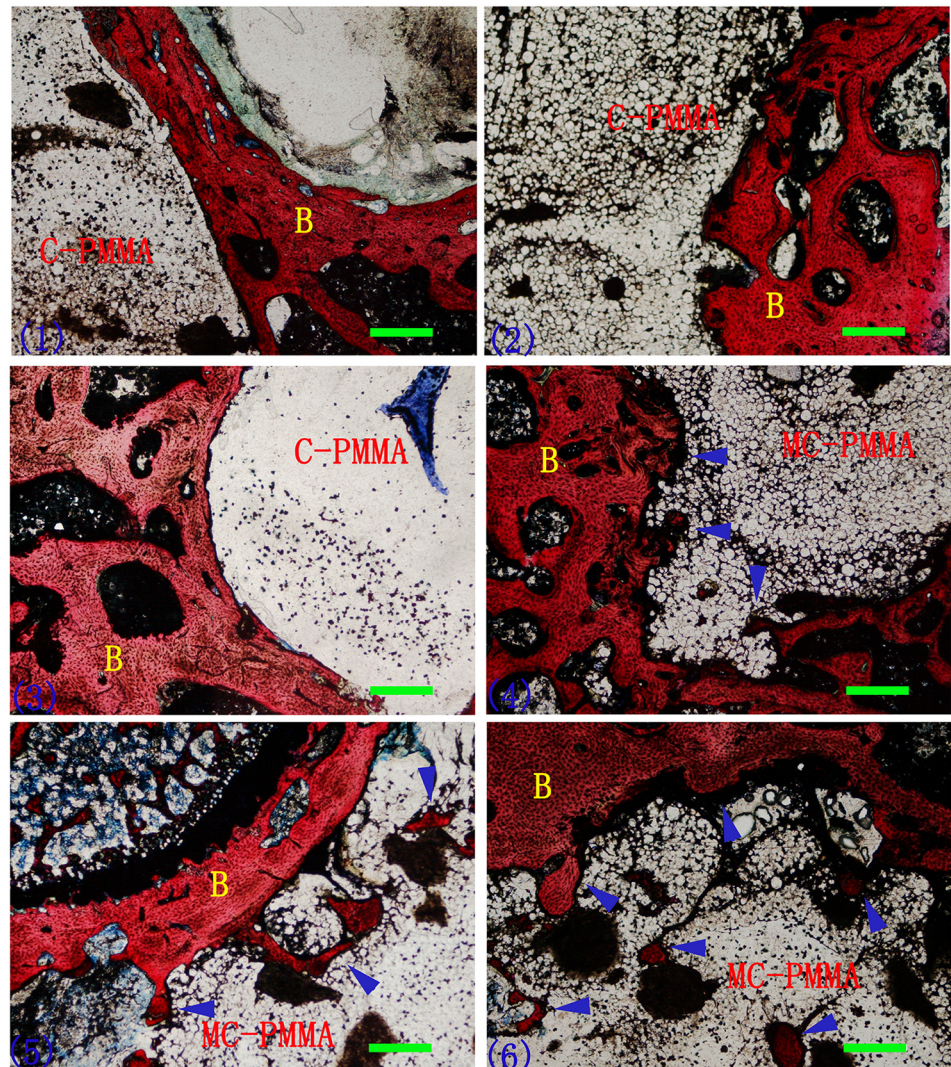
Fig 3. Van Gieson surface staining of C-PMMA (1–3) and MC-PMMA (4–6) after implantation for 4 (1,4), 12 (2, 5) and 24 weeks (3, 6). Blue arrow indicates the insertion site of bone tissue; B, bone; Bar = 400μm.

doi:10.1371/journal.pone.0129018.g003

results in stress shielding and implant loosening[40, 41]. MC-PMMA exhibited excellent operatingperformance and compressive strength. In addition, the elastic modulus of MC-PMMA (15%, wt/wt) was reduced from 1.91±0.08GPa to 1.21±0.12GPa, which was closer to that of cancellous bone (0.05–0.5GPa)[42].

Compared with various bioactive substitute materials such as HA and AWG, MC-PMMA had a greater advantage in its elastic modulus (Table 2). In addition, many PMMA-based bioactive cements have been developed. In contrast, the Ti-PMMA developed by Fukuda C *et al* had sufficient compressive strength but a high elastic modulus[43]. The HEMA-PMMA developed by Wolf-Brandstetter C, The HA-chitin-PMMA developed by Kim SB and the TCP-PMMA developed by Vazquez B all showed reductions both in compressive strength and elastic modulus[44–46].
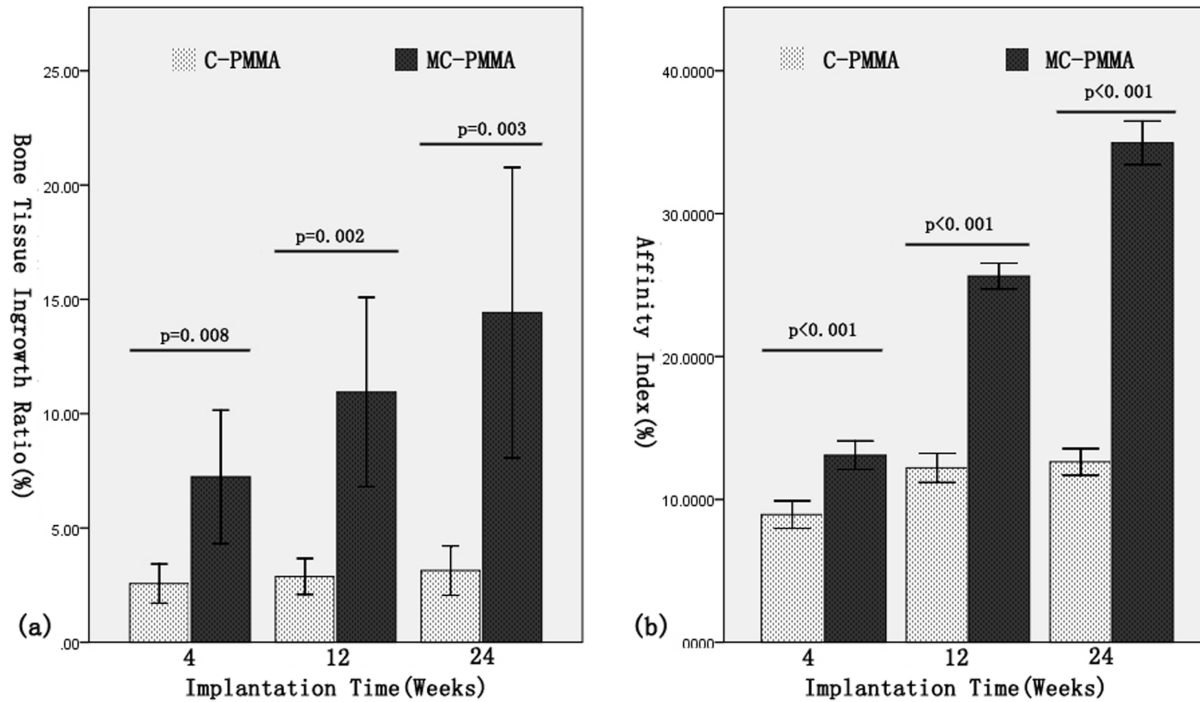
Fig 4. Bone tissue ingrowth ratio (A) and affinity index (B) for all the tested cements for 4, 12 and 24 weeks. $\overline{X}$ ±SD, n = 9. (A) The bone tissue ingrowth ratios in MC-PMMA were significantly higher than that of C-PMMA group (p<0.05). (B) The bone affinity indexes (AI) in MC-PMMA were significantly higher than that of C-PMMA group (p<0.05).

doi:10.1371/journal.pone.0129018.g004

Biosafety

Biosafety is a prerequisite for bone substitute materials *in vivo* applications. In accordance with the international standards ISO 10993[37], the MC-PMMA bone cement was biologically safe in cytotoxicity and proliferation assays and with respect to blood compatibility, local reaction after implantation, acute systemic toxicity and chronic liver and kidney toxicity.

Previous studies of MC have shown no toxic effects[26]. The toxicity of bone cement is mainly due to the toxicity of its components and of unpolymerized monomer. Adding MC to the PMMA component did not increase the toxicity, indicating that there were no significant effects of MC on PMMA polymerization.

Because bone cement will remain in the body for long periods, the long-term toxicity of MC-PMMA applications requires further evaluation.

Biocompatibility with bone tissue

Interface morphology. Charnley and Willert studied the interfacial histological reaction in the 1970s and discovered a pearl-like layer between bone cement and bone[1, 47]. Draenert and Linder then revealed that this layer was demineralized bone tissue with dense connective tissue in the inner layer[2, 48]. These findings are consistent with the histological features observed in our study (Fig 3). Both C-PMMA and MC-PMMA showed connective tissues between the bone structure and the bone cement.

The formation of connective tissue is related to cement shrinkage that occurs during the polymerization reaction. A study by Muller *et al.* found a volume change of 2–6% during shrinkage[49], which produced voids in the interface. The existence of voids caused slight
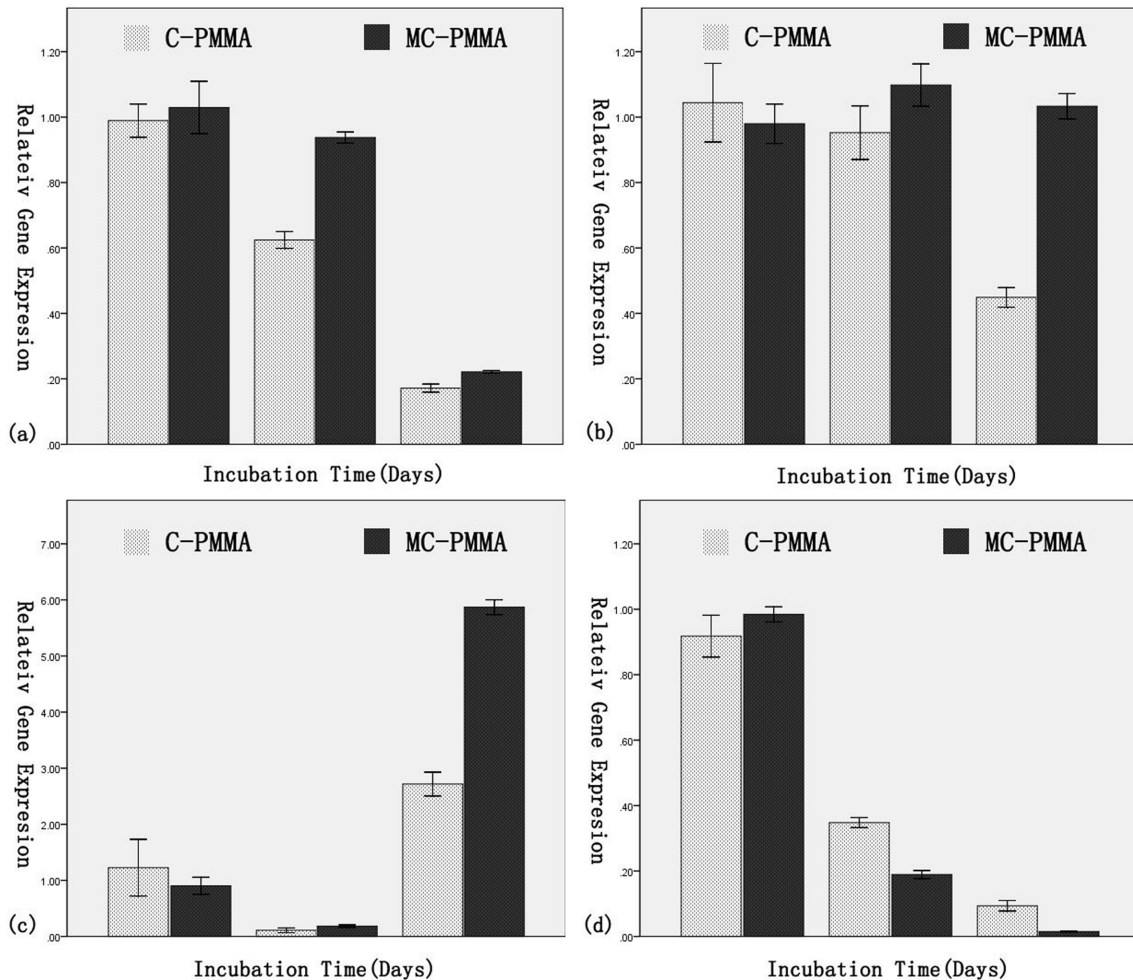
Fig 5. Real-time PCR analysis of osteogenic gene markers expression of MG63 cell line grown in the surface of C-PMMA and MC-PMMA after 1, 7 and 14 days. (a) Osteonectin (SPARC) (b) Collagen-1 (Col1A1) (c) Bone sialoprotein (IBSP) and (d) Osteocalcin (BGLAP). Expression normalized to housekeeping gene ACTIN. X±SD, n = 3, p<0.05.

doi:10.1371/journal.pone.0129018.g005

movement and absorption in the interface and ultimately induced the formation of a layer of dense connective tissue. It was difficult to avoid the formation of connective tissue.

Interface osteonecrosis. Bone tissue necrosis usually occurs after implantation of PMMA bone cement. The necrosis is caused mainly by the exothermic polymerization reaction and by the toxicity of MMA monomers[3].

In our study, both C-PMMA and MC-PMMA caused apparent tissue necrosis. This result indicated no significant effect of MC on PMMA polymerization or the exothermic reaction. However, the extent of the exothermic reaction was volume-related. Stanczyk *et al* revealed that the interface would produce a high temperature above 70°C only when the implanted volume exceeded 10% of the bone tissue volume[50]. Boner *et al.* found that the thermal necrosis risk increased only when the implanted PMMA thickness exceeded 5mm and the volume exceeded 6cc[51]. In our study, the implanted bone cement was less than 1cc in volume and less than 5mm in thickness.

Interface crosslinking. Interface crosslinking has been the greatest concern in materials research. In our study, we observed more bone tissue ingrowth into the bone cement to form

Table 2. Mechanical properties of different materials.

Author	Material	Strength(MPa)	Elastic modulus(GPa)
Ascenzi A[71, 72]	Osteon	102–120	5.5–12
Rho JY[73]	Trabecular	-	1–20
Kokubo T[42]	Cancellous bone	2–12	0.05–0.5
	Cortical bone	100–230	7–30
	Bioglass(45S5)	-	35
	HA	500–1000	80–110
	Apatite-and wollastonite-containing glass (AWG)	1080	118
Fukuda C[43]	Ti-PMMA	126.5–130.0	3.45–4.19
Wolf-Brandstetter C[44]	HEMA-PMMA	75–80	1.3–1.4
Kim SB[45]	HA- chitin-PMMA	48.8–81.8	1.5–2.4
Vazquez B[46]	TCP-PMMA	76–80	1.4–1.6
Our Study	MC-PMMA	89.30±5.26	1.21±0.12
	PMMA	90.53±4.39	1.91±0.08

doi:10.1371/journal.pone.0129018.t002

tight crosslinking, and the bone ingrowth ratio gradually increased with the duration of implant residence. After 24 weeks, the bone ingrowth ratio in the MC-PMMA group was four times that in the C-PMMA group (Fig 4).

Many studies of PMMA-based cements have attempted to enhance interface crosslinking. Current research ideas mainly include three strategies: (a) adding partially biodegradable materials, such as polyhydroxyalkenonate (PHA) and poly-β-hydroxybutyrate (PHB)[52, 53]; (b) adding completely biodegradable materials to commercial PMMA or modified PMMA, such as sodium fluoride[54, 55], nanoscale aluminum oxide (average size of 70nm)[56], cellulose[57, 58] and tricalcium phosphate ceramic (TCP)[59]; and (c) adding bioactive materials to commercial PMMA or modified PMMA, such as apatite wollastonite glass (AWG)[60, 61], hydroxyapatite (HA) [62, 63] and recombinant growth factor [64]. In all of these studies, the formation of pores and the induction and adsorption properties were responsible for improvements in interface crosslinking.

We compared the bone affinity index 12 weeks after implantation with representative PMMA-based studies. He Q *et al.* investigated porous PMMA bone cement created by adding cellulose, which resulted in a bone affinity index of 13.95%[65]. Goto K *et al.* investigated PMMA with the addition of titanium, indicating a bone affinity index of 11.0%[66]. Wong CT *et al.* investigated strontium and HA composited PMMA, which showed a bone affinity index that increased to 73.55%[22].

Because of the poor biological activity of PMMA, there have also been a large number of studies investigating non-PMMA-based bone cement. Kaili *et al.* studied the implantation of calcium silicate bioactive bone cement with the addition of strontium, which showed a 4.4% increase in the bone mass after 4 weeks[67]. Ulrich *et al.* investigated calcium phosphate bone cement with the addition of strontium, which showed a 6.8% increase of the bone mineralization proportion after 6 weeks of implantation[68].

MC-PMMA showed better biological activity than any of the above studies, with the exception of Sr-HA-PMMA. It was reasonable for MC to be biodegradable[26, 32], thereby forming a porous surface and thus providing a bone tissue growth scaffold. On the other hand, gene expression analysis showed increases in IBSP, SPARC and Col1A1 and decreases in BGLAP in the MC-PMMA group (Fig 5), indicating osteoinductive activity.

IBSP, SPARC, Col1A1 and BGLAP genes are expressed during proliferation and mineralization in osteocytes. Owen TA and Jääskeläinen T revealed that BGLAP expression decreased

only during proliferation by Fos-Jun inhibition[69, 70]. It is thus reasonable to speculate that the impact of MC-PMMA on osteogenic activity is mainly to promote proliferation.

The pore formation and osteogenic activity of MC-PMMA might be involved in cement-bone interface integration; however, further studies are needed to investigate MC-PMMA porosity before and after implantation.

Conclusions

PMMA bone cement with the addition of nano-HA-coated bone collagen showed superior mechanical properties, good biosafety and excellent biocompatibility with bone tissues. MC-PMMA (15.0%(wt) impregnated) significantly lowered the compressive modulus of PMMA from 1.91GPa to 1.21GPa while having little effect on its compressive strength and solidification, which could reduce the risk of aseptic loosening. In accordance with the international standard ISO 10993, MC-PMMA bone cement was biologically safe in cytotoxicity and proliferation assays and with respect to blood compatibility, local reaction after implantation, acute systemic toxicity and chronic liver and kidney toxicity. In addition, the bone-cement interface crosslinking was significantly higher for MC-PMMA than for C-PMMA 6 months after implantation in the distal femur of rabbits. A comparison of gene expression between the MC-PMMA and C-PMMA groups also suggested that MC-PMMA might improve osteogenic bioactivity. We propose that PMMA bone cement withadded nano-HA-coated bone collagen has profound clinical values.

Supporting Information

S1 Fig. The growth state in 24h and 5 days after L929 cell subculture. 1–4 was the growth state in 24h and 5–8 was for 5 days. The arrow indicated dead cells and no cell necrosis occurred in NC, MC-PMMA, C-PMMA groups. Phase contrast microscope (Olympus, Japan), 20×. NC: Negative Control; PC: Positive Control; MC-PMMA: Mineralized Collagen PMMA Bone Cement; C-PMMA: Classical PMMA Bone Cement.
(TIF)

S2 Fig. HE staining of mice liver (1,2) and kidney (3, cortex; 4, medulla) after intraperitoneal injection of material extracts for 72 hours. 1, 10×; 2–4, 20×.
(TIF)

S3 Fig. HE staining of local muscle after implantation of MC-PMMA for 1 (1), 4 (2), 7 (3), 12 (4) and 26 (5) weeks. Bar = 100μm; M, muscle; white arrow, inflammatory cells; black arrow, connective tissue.
(TIF)

S4 Fig. HE staining of rat liver (1,2) and kidney (3, cortex; 4, medulla) after implantation of MC-PMMA in the gluteus maximus for 12 weeks. 1, 10×; 2–4, 20×.
(TIF)

S1 Table. Information of gene primers.
(DOCX)

S2 Table. The cell relative growth rate (RGR) with CKK8 method in different periods after cell subculture ($\overline{X} \pm$ SD (CTS), n = 6, %).
(DOCX)

S3 Table. The absorbance at 545nm wavelength (OD545) and hemolysis ratio ($\overline{X} \pm$ SD, n = 6).
(DOCX)

S4 Table. Weight change after intraperitoneal injection of material extracts (gram, $\overline{X}$ ±SD, n = 15).
(DOCX)

Acknowledgments

The authors wish to thank Imaging center of Animal Medical Research Institute of Chinese Academe of Medicine for providing the micro-CT imaging instrument, training and general support.

Author Contributions

Conceived and designed the experiments: TL XW YB LZ FC ZQ. Performed the experiments: TL LZ ZQ. Analyzed the data: TL LZ YB ZQ. Contributed reagents/materials/analysis tools: TL XW YB LZ FC ZQ. Wrote the paper: TL LZ.

References

1. Charnley J. The reaction of bone to self-curing acrylic cement. A long-term histological study in man. The Journal of bone and joint surgery British volume. 1970; 52(2):340–53. Epub 1970/05/01. PMID: 5445416.

2. Draenert K. The John Charnley Award Paper. Histomorphology of the bone-to-cement interface: remodeling of the cortex and revascularization of the medullary canal in animal experiments. The Hip. 1981:71–110. Epub 1981/01/01. PMID: 7333896.

3. Feith R. Side-effects of acrylic cement implanted into bone. A histologicl, (micro)angiographic, fluorescence-microscopic and autoradiog-aphic study in the rabbit femur. Acta orthopaedica Scandinavica Supplementum. 1975; 161:3–136. Epub 1975/01/01. PMID: 1062111.

4. Bauer TW, Smith ST. Bioactive materials in orthopaedic surgery: overview and regulatory considerations. Clinical orthopaedics and related research. 2002;(395:):11–22. Epub 2002/04/09. PMID: 11937862.

5. Muijs SP, van Erkel AR, Dijkstra PD. Treatment of painful osteoporotic vertebral compression fractures: a brief review of the evidence for percutaneous vertebroplasty. The Journal of bone and joint surgery British volume. 2011; 93(9):1149–53. Epub 2011/09/14. doi: 10.1302/0301-620x.93b9.26152 PMID: 21911522.

6. Brown TE, Harper BL, Bjorgul K. Comparison of cemented and uncemented fixation in total knee arthroplasty. Orthopedics. 2013; 36(5):380–7. Epub 2013/05/16. doi: 10.3928/01477447-20130426-10 PMID: 23672897.

7. Zwartele R, Poll RG. Cemented total hip arthroplasty in rheumatoid arthritis. A systematic review of the literature. Hip international: the journal of clinical and experimental research on hip pathology and therapy. 2013; 23(2):111–22. Epub 2013/05/01. doi: 10.5301/hip.2013.11049 PMID: 23629816.

8. Zuo D, Zheng L, Sun W, Fu D, Hua Y, Cai Z. Contemporary adjuvant polymethyl methacrylate cementation optimally limits recurrence in primary giant cell tumor of bone patients compared to bone grafting: a systematic review and meta-analysis. World journal of surgical oncology. 2013; 11:156. Epub 2013/07/23. doi: 10.1186/1477-7819-11-156 PMID: 23866921; PubMed Central PMCID: PMCPmc3717274.

9. Scolaro JA, Lackman RD. Surgical management of metastatic long bone fractures: principles and techniques. The Journal of the American Academy of Orthopaedic Surgeons. 2014; 22(2):90–100. Epub 2014/02/04. doi: 10.5435/jaaos-22-02-90 PMID: 24486755.

10. Parker MJ, Gurusamy KS, Azegami S. Arthroplasties (with and without bone cement) for proximal femoral fractures in adults. The Cochrane database of systematic reviews. 2010;(6:):Cd001706. Epub 2010/06/18. doi: 10.1002/14651858.CD001706.pub4 PMID: 20556753.

11. Jamsen E, Eskelinen A, Peltola M, Makela K. High Early Failure Rate After Cementless Hip Replacement in the Octogenarian. Clinical orthopaedics and related research. 2014. Epub 2014/04/29. doi: 10.1007/s11999-014-3641-7 PMID: 24771260.

12. Makela KT, Matilainen M, Pulkkinen P, Fenstad AM, Havelin L, Engesaeter L, et al. Failure rate of cemented and uncemented total hip replacements: register study of combined Nordic database of four nations. BMJ (Clinical research ed). 2014; 348:f7592. Epub 2014/01/15. doi: 10.1136/bmj.f7592 PMID: 24418635.

13. Sadoghi P, Liebensteiner M, Agreiter M, Leithner A, Bohler N, Labek G. Revision surgery after total joint arthroplasty: a complication-based analysis using worldwide arthroplasty registers. The Journal of arthroplasty. 2013; 28(8):1329–32. Epub 2013/04/23. doi: 10.1016/j.arth.2013.01.012 PMID: 23602418.

14. Savarino L, Stea S, Ciapetti G, Paganetto G, Donati ME, Alvergna P, et al. Microstructural investigation of bone-cement interface. Journal of biomedical materials research. 1995; 29(6):701–5. Epub 1995/06/01. doi: 10.1002/jbm.820290605 PMID: 7593006.

15. Funk MJ, Litsky AS. Effect of cement modulus on the shear properties of the bone-cement interface. Biomaterials. 1998; 19(17):1561–7. Epub 1998/11/27. PMID: 9830981.

16. Litsky AS, Rose RM, Rubin CT, Thrasher EL. A reduced-modulus acrylic bone cement: preliminary results. Journal of orthopaedic research: official publication of the Orthopaedic Research Society. 1990; 8(4):623–6. Epub 1990/07/01. doi: 10.1002/jor.1100080420 PMID: 2355302.

17. Kolb JP, Kueny RA, Puschel K, Boger A, Rueger JM, Morlock MM, et al. Does the cement stiffness affect fatigue fracture strength of vertebrae after cement augmentation in osteoporotic patients? European spine journal: official publication of the European Spine Society, the European Spinal Deformity Society, and the European Section of the Cervical Spine Research Society. 2013; 22(7):1650–6. Epub 2013/05/17. doi: 10.1007/s00586-013-2809-2 PMID: 23677522; PubMed Central PMCID: PMCPmc3698342.

18. Hedia HS, Abdl-Shafi AA, Fouda N. The effect of elastic modulus of the backing material on the fatigue notch factor and stress. Bio-medical materials and engineering. 2000; 10(3–4):141–56. Epub 2001/02/24. PMID: 11202144.

19. Lam WM, Pan HB, Fong MK, Cheung WS, Wong KL, Li ZY, et al. In Vitro characterization of low modulus linoleic acid coated strontium-substituted hydroxyapatite containing PMMA bone cement. Journal of biomedical materials research Part B, Applied biomaterials. 2011; 96(1):76–83. Epub 2010/11/06. doi: 10.1002/jbm.b.31741 PMID: 21053263.

20. Kinzl M, Benneker LM, Boger A, Zysset PK, Pahr DH. The effect of standard and low-modulus cement augmentation on the stiffness, strength, and endplate pressure distribution in vertebroplasty. European spine journal: official publication of the European Spine Society, the European Spinal Deformity Society, and the European Section of the Cervical Spine Research Society. 2012; 21(5):920–9. Epub 2011/12/16. doi: 10.1007/s00586-011-2119-5 PMID: 22170449; PubMed Central PMCID: PMCPmc3337907.

21. Hench LL, Thompson I. Twenty-first century challenges for biomaterials. Journal of the Royal Society, Interface / the Royal Society. 2010; 7 Suppl 4:S379–91. Epub 2010/05/21. doi: 10.1098/rsif.2010.0151.focus PMID: 20484227; PubMed Central PMCID: PMCPmc2943892.

22. Wong CT, Lu WW, Chan WK, Cheung KM, Luk KD, Lu DS, et al. In vivo cancellous bone remodeling on a strontium-containing hydroxyapatite (sr-HA) bioactive cement. Journal of biomedical materials research Part A. 2004; 68(3):513–21. Epub 2004/02/06. doi: 10.1002/jbm.a.20089 PMID: 14762931.

23. Goto K, Shinzato S, Fujibayashi S, Tamura J, Kawanabe K, Hasegawa S, et al. The biocompatibility and osteoconductivity of a cement containing beta-TCP for use in vertebroplasty. Journal of biomedical materials research Part A. 2006; 78(3):629–37. Epub 2006/06/22. doi: 10.1002/jbm.a.30793 PMID: 16788976.

24. Mattila RH, Laurila P, Rekola J, Gunn J, Lassila LV, Mantyla T, et al. Bone attachment to glass-fibre-reinforced composite implant with porous surface. Acta biomaterialia. 2009; 5(5):1639–46. Epub 2009/03/10. doi: 10.1016/j.actbio.2009.01.020 PMID: 19268643.

25. Miller MA, Goodheart JR, Izant TH, Rimnac CM, Cleary RJ, Mann KA. Loss of cement-bone interlock in retrieved tibial components from total knee arthroplasties. Clinical orthopaedics and related research. 2014; 472(1):304–13. Epub 2013/08/27. doi: 10.1007/s11999-013-3248-4 PMID: 23975251; PubMed Central PMCID: PMCPmc3889460.

26. Liao SS, Guan K, Cui FZ, Shi SS, Sun TS. Lumbar spinal fusion with a mineralized collagen matrix and rhBMP-2 in a rabbit model. Spine. 2003; 28(17):1954–60. Epub 2003/09/16. doi: 10.1097/01.brs.0000083240.13332.f6 PMID: 12973141.

27. Lian K, Lu H, Guo X, Cui F, Qiu Z, Xu S. The mineralized collagen for the reconstruction of intra-articular calcaneal fractures with trabecular defects. Biomatter. 2013; 3(4). Epub 2013/11/26. doi: 10.4161/biom.27250 PMID: 24270815; PubMed Central PMCID: PMCPmc3903599.

28. Liu X, Wang XM, Chen Z, Cui FZ, Liu HY, Mao K, et al. Injectable bone cement based on mineralized collagen. Journal of biomedical materials research Part B, Applied biomaterials. 2010; 94(1):72–9. Epub 2010/03/26. doi: 10.1002/jbm.b.31625 PMID: 20336741.

29. Liu HY, Liu X, Zhang LP, Ai HJ, Cui FZ. Improvement on the performance of bone regeneration of calcium sulfate hemihydrate by adding mineralized collagen. Tissue engineering Part A. 2010; 16(6):2075–84. Epub 2010/02/09. doi: 10.1089/ten.TEA.2009.0669 PMID: 20136401.

30. Liu J, Mao K, Liu Z, Wang X, Cui F, Guo W, et al. Injectable biocomposites for bone healing in rabbit femoral condyle defects. PloS one. 2013; 8(10):e75668. Epub 2013/10/23. doi: 10.1371/journal.pone.0075668 PMID: 24146770; PubMed Central PMCID: PMCPmc3797737.

31. Liu X, Liu HY, Lian X, Shi XL, Wang W, Cui FZ, et al. Osteogenesis of mineralized collagen bone graft modified by PLA and calcium sulfate hemihydrate: in vivo study. Journal of biomaterials applications. 2013; 28(1):12–9. Epub 2012/01/26. doi: 10.1177/0885328211433618 PMID: 22274876.

32. Liao SS, Cui FZ. In vitro and in vivo degradation of mineralized collagen-based composite scaffold: nanohydroxyapatite/collagen/poly(L-lactide). Tissue engineering. 2004; 10(1–2):73–80. Epub 2004/03/11. doi: 10.1089/107632704322791718 PMID: 15009932.

33. Li J, Hong J, Zheng Q, Guo X, Lan S, Cui F, et al. Repair of rat cranial bone defects with nHAC/PLLA and BMP-2-related peptide or rhBMP-2. Journal of orthopaedic research: official publication of the Orthopaedic Research Society. 2011; 29(11):1745–52. Epub 2011/04/19. doi: 10.1002/jor.21439 PMID: 21500252.

34. Hao W, Dong J, Jiang M, Wu J, Cui F, Zhou D. Enhanced bone formation in large segmental radial defects by combining adipose-derived stem cells expressing bone morphogenetic protein 2 with nHA/RHLC/PLA scaffold. International orthopaedics. 2010; 34(8):1341–9. Epub 2010/02/09. doi: 10.1007/s00264-009-0946-3 PMID: 20140671; PubMed Central PMCID: PMCPmc2989079.

35. ISO 5833:2002 I. Implants for surgery – Acrylic resin cements.

36. ASTM C191 A. Standard Test Methods for Time of Setting of Hydraulic Cement by Vicat Needle. 10.1520/C0191.

37. ISO 10993 I. Biological evaluation of medical devices.

38. Hayashi K, Uenoyama K, Matsuguchi N, Nakagawa S, Sugioka Y. The affinity of bone to hydroxyapatite and alumina in experimentally induced osteoporosis. The Journal of arthroplasty. 1989; 4(3):257–62. Epub 1989/09/01. PMID: 2552019.

39. F451 A. Standard Specification for Acrylic Bone Cement.

40. Beall DP, Datir A, D'Souza SL, D'Souza LS, Gunda D, Morelli J, et al. Percutaneous treatment of insufficiency fractures: principles, technique and review of literature. Skeletal radiology. 2010; 39(2):117–30. Epub 2009/06/09. doi: 10.1007/s00256-009-0722-x PMID: 19504091.

41. Driscoll M, Blyum L. The presence of physiological stress shielding in the degenerative cycle of musculoskeletal disorders. Journal of bodywork and movement therapies. 2011; 15(3):335–42. Epub 2011/06/15. doi: 10.1016/j.jbmt.2010.05.002 PMID: 21665110.

42. Kokubo T, Kim HM, Kawashita M. Novel bioactive materials with different mechanical properties. Biomaterials. 2003; 24(13):2161–75. Epub 2003/04/18. PMID: 12699652.

43. Fukuda C, Goto K, Imamura M, Nakamura T. Bioactive bone cement with a low content of titania particles without postsilanization: effect of filler content on osteoconductivity, mechanical properties, and handling characteristics. Journal of biomedical materials research Part B, Applied biomaterials. 2010; 95(2):407–13. Epub 2010/09/23. doi: 10.1002/jbm.b.31731 PMID: 20860047.

44. Wolf-Brandstetter C, Roessler S, Storch S, Hempel U, Gbureck U, Nies B, et al. Physicochemical and cell biological characterization of PMMA bone cements modified with additives to increase bioactivity. Journal of biomedical materials research Part B, Applied biomaterials. 2013; 101(4):599–609. Epub 2013/01/03. doi: 10.1002/jbm.b.32862 PMID: 23281256.

45. Kim SB, Kim YJ, Yoon TL, Park SA, Cho IH, Kim EJ, et al. The characteristics of a hydroxyapatite-chitosan-PMMA bone cement. Biomaterials. 2004; 25(26):5715–23. Epub 2004/05/19. doi: 10.1016/j.biomaterials.2004.01.022 PMID: 15147817.

46. Vazquez B, Ginebra MP, Gil X, Planell JA, San Roman J. Acrylic bone cements modified with beta-TCP particles encapsulated with poly(ethylene glycol). Biomaterials. 2005; 26(20):4309–16. Epub 2005/02/03. doi: 10.1016/j.biomaterials.2004.10.042 PMID: 15683655.

47. Willert HG, Puls P. [The reaction of bone to bone-cement in the replacement of the hip joint]. Archiv fur orthopadische und Unfall-Chirurgie. 1972; 72(1):33–71. Epub 1972/01/01. PMID: 5020683.

48. Linder L, Hansson HA. Ultrastructural aspects of the interface between bone and cement in man. Report of three cases. The Journal of bone and joint surgery British volume. 1983; 65(5):646–9. Epub 1983/11/01. PMID: 6643571.

49. Muller SD, Green SM, McCaskie AW. The dynamic volume changes of polymerising polymethyl methacrylate bone cement. Acta orthopaedica Scandinavica. 2002; 73(6):684–7. Epub 2003/01/30. doi: 10.1080/000164702321039688 PMID: 12553519.

50. Stanczyk M, van Rietbergen B. Thermal analysis of bone cement polymerisation at the cement-bone interface. Journal of biomechanics. 2004; 37(12):1803–10. Epub 2004/11/03. doi: 10.1016/j.jbiomech.2004.03.002 PMID: 15519587.

51. Boner V, Kuhn P, Mendel T, Gisep A. Temperature evaluation during PMMA screw augmentation in osteoporotic bone–an in vitro study about the risk of thermal necrosis in human femoral heads. Journal of biomedical materials research Part B, Applied biomaterials. 2009; 90(2):842–8. Epub 2009/04/09. doi: 10.1002/jbm.b.31353 PMID: 19353575.

52. Nguyen S, Marchessault RH. Graft copolymers of methyl methacrylate and poly([R]-3-hydroxybutyrate) macromonomers as candidates for inclusion in acrylic bone cement formulations: Compression testing. Journal of biomedical materials research Part B, Applied biomaterials. 2006; 77(1):5–12. Epub 2005/10/06. doi: 10.1002/jbm.b.30430 PMID: 16206205.

53. Nguyen S, Marchessault RH. Synthesis and properties of graft copolymers based on poly(3-hydroxybutyrate) macromonomers. Macromolecular bioscience. 2004; 4(3):262–8. Epub 2004/10/07. doi: 10.1002/mabi.200300088 PMID: 15468216.

54. Minari C, Baleani M, Cristofolini L, Baruffaldi F. The effect on the fatigue strength of bone cement of adding sodium fluoride. Proceedings of the Institution of Mechanical Engineers Part H, Journal of engineering in medicine. 2001; 215(2):251–3. Epub 2001/05/31. PMID: 11382084.

55. Minari C, Cristofolini L, Baruffaldi F, Pierotti L. Radiopacity and fatigue characterization of a novel acrylic bone cement with sodium fluoride. Artificial organs. 2000; 24(9):751–7. Epub 2000/09/30. PMID: 11012547.

56. Gomoll AH, Fitz W, Scott RD, Thornhill TS, Bellare A. Nanoparticulate fillers improve the mechanical strength of bone cement. Acta orthopaedica. 2008; 79(3):421–7. Epub 2008/07/16. doi: 10.1080/17453670710015349 PMID: 18622848.

57. Liu YK, Park JB, Njus GO, Stienstra D. Bone-particle-impregnated bone cement: an in vitro study. Journal of biomedical materials research. 1987; 21(2):247–61. Epub 1987/02/01. doi: 10.1002/jbm.820210208 PMID: 3818684.

58. Williams JL, Johnson WJ. Elastic constants of composites formed from PMMA bone cement and anisotropic bovine tibial cancellous bone. Journal of biomechanics. 1989; 22(6–7):673–82. Epub 1989/01/01. PMID: 2808448.

59. Canul-Chuil A, Vargas-Coronado R, Cauich-Rodriguez JV, Martinez-Richa A, Fernandez E, Nazhat SN. Comparative study of bone cements prepared with either HA or alpha-TCP and functionalized methacrylates. Journal of biomedical materials research Part B, Applied biomaterials. 2003; 64(1):27–37. Epub 2002/12/11. doi: 10.1002/jbm.b.10486 PMID: 12474244.

60. Shinzato S, Nakamura T, Kokubo T, Kitamura Y. A new bioactive bone cement: effect of glass bead filler content on mechanical and biological properties. Journal of biomedical materials research. 2001; 54(4):491–500. Epub 2001/06/28. PMID: 11426593.

61. Shinzato S, Nakamura T, Kokubo T, Kitamura Y. Bioactive bone cement: effect of filler size on mechanical properties and osteoconductivity. Journal of biomedical materials research. 2001; 56(3):452–8. Epub 2001/05/24. PMID: 11372064.

62. Saito M, Maruoka A, Mori T, Sugano N, Hino K. Experimental studies on a new bioactive bone cement: hydroxyapatite composite resin. Biomaterials. 1994; 15(2):156–60. Epub 1994/01/01. PMID: 8011863.

63. Jager M, Wilke A. Comprehensive biocompatibility testing of a new PMMA-hA bone cement versus conventional PMMA cement in vitro. Journal of biomaterials science Polymer edition. 2003; 14(11):1283–98. Epub 2004/02/11. PMID: 14768914.

64. Goodwin CJ, Braden M, Downes S, Marshall NJ. Investigation into the release of bioactive recombinant human growth hormone from normal and low-viscosity poly(methylmethacrylate) bone cements. Journal of biomedical materials research. 1997; 34(1):47–55. Epub 1997/01/01. PMID: 8978652.

65. He Q, Chen H, Huang L, Dong J, Guo D, Mao M, et al. Porous surface modified bioactive bone cement for enhanced bone bonding. PloS one. 2012; 7(8):e42525. Epub 2012/08/21. doi: 10.1371/journal.pone.0042525 PMID: 22905143; PubMed Central PMCID: PMCPmc3414445.

66. Goto K, Tamura J, Shinzato S, Fujibayashi S, Hashimoto M, Kawashita M, et al. Bioactive bone cements containing nano-sized titania particles for use as bone substitutes. Biomaterials. 2005; 26(33):6496–505. Epub 2005/06/09. doi: 10.1016/j.biomaterials.2005.04.044 PMID: 15941580.

67. Lin K, Xia L, Li H, Jiang X, Pan H, Xu Y, et al. Enhanced osteoporotic bone regeneration by strontium-substituted calcium silicate bioactive ceramics. Biomaterials. 2013; 34(38):10028–42. Epub 2013/10/08. doi: 10.1016/j.biomaterials.2013.09.056 PMID: 24095251.

68. Thormann U, Ray S, Sommer U, Elkhassawna T, Rehling T, Hundgeburth M, et al. Bone formation induced by strontium modified calcium phosphate cement in critical-size metaphyseal fracture defects in ovariectomized rats. Biomaterials. 2013; 34(34):8589–98. Epub 2013/08/03. doi: 10.1016/j.biomaterials.2013.07.036 PMID: 23906515.

69. Islas-Blancas ME, Cervantes JM, Vargas-Coronado R, Cauich-Rodriguez JV, Vera-Graziano R, Martinez-Richa A. Characterization of bone cements prepared with functionalized methacrylates and

hydroxyapatite. Journal of biomaterials science Polymer edition. 2001; 12(8):893–910. Epub 2001/11/23. PMID: 11718483.

70. Deb S, Braden M, Bonfield W. Water absorption characteristics of modified hydroxyapatite bone cements. Biomaterials. 1995; 16(14):1095–100. Epub 1995/09/01. PMID: 8519931.

71. Ascenzi A, Bonucci E. The tensile properties of single osteons. The Anatomical record. 1967; 158 (4):375–86. Epub 1967/08/01. doi: 10.1002/ar.1091580403 PMID: 4861577.

72. Ascenzi A, Bonucci E. The compressive properties of single osteons. The Anatomical record. 1968; 161(3):377–91. Epub 1968/07/01. doi: 10.1002/ar.1091610309 PMID: 4879362.

73. Rho JY, Ashman RB, Turner CH. Young's modulus of trabecular and cortical bone material: ultrasonic and microtensile measurements. Journal of biomechanics. 1993; 26(2):111–9. Epub 1993/02/01. PMID: 8429054.